Macromolecules

Article

Cite This: Macromolecules 2019, 52, 4713−4720

pubs.acs.org/Macromolecules

Phosphazene Base-Mediated Azide−Alkyne Click Polymerization toward 1,5-Regioregular Polytriazoles

Baixue Li,[†] Yong Liu,[†] Han Nie,[†] Anjun Qin,*[,†] and Ben Zhong Tang*[,†,‡]

[†]State Key Laboratory of Luminescent Materials and Devices, Center for Aggregation-Induced Emission, South China University of Technology, Guangzhou 510640, China

[‡]Department of Chemistry, Hong Kong Branch of Chinese National Engineering Research Center for Tissue Restoration and Reconstruction, Institute for Advanced Study, and Department of Chemical and Biological Engineering, The Hong Kong University of Science & Technology, Clear Water Bay, Kowloon, Hong Kong, China

Supporting Information

ABSTRACT: Cu(I)-catalyzed azide−alkyne click polymerization has become a powerful tool for the construction of 1,4-regioregular polytriazoles (PTAs). However, the polymerization toward the synthesis of 1,5-regioregular PTAs has been rarely reported, and the structure−property relationship between 1,5- and 1,4-regioregular PTAs needs to be studied further. In this work, an efficient superbase of phosphazene base (*t*-BuP_4)-mediated azide−alkyne click polymerization was developed, and soluble and thermally stable 1,5-regioregular PTAs with high molecular weights (M_w up to 26 600) were generated in high yields (up to 99%). The relationship between the regiostructures and the thermal stability, light refractivity, photophysical properties, electrochemical behaviors of PTAs was investigated, and the results indicate that the 1,4-regioregular PTA exhibits better conjugation and planarity than that of the 1,5-regioregular one. Thus, this work not only develops a powerful *t*-BuP_4-mediated azide−alkyne click polymerization for the preparation of 1,5-regioregular PTAs but also provides a platform for investigating the structure−property relationship of PTAs, which will guide the design of new PTAs for diverse applications.

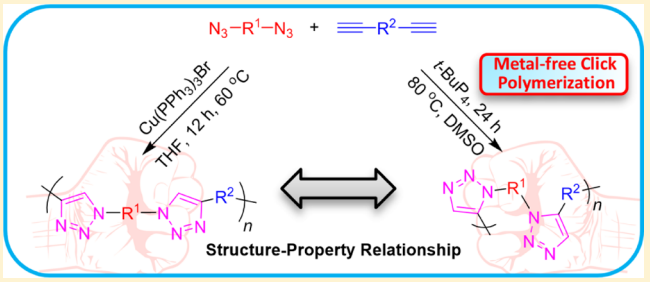

INTRODUCTION

The exploration of facile and effective polymerization is of utmost importance for polymer science.[1−6] Generally, new polymerizations are developed based on the elegant organic reactions that enjoy the features of high efficiency, regioselectivity, tolerance toward functionality, wide scope of monomers, mild reaction conditions, and so on. The click reactions well meet these criteria,[7−13] and some of them have been developed into efficient click polymerizations. Thereinto, the Cu(I)-catalyzed azide−alkyne click polymerization (AACP) is the representative, from which plenteous linear and hyperbranched 1,4-regioregular polytriazoles (PTAs) with advanced properties have been produced.[14−28] Notably, the Ru(II)-catalyzed AACP that readily furnishes 1,5-regioregular PTAs has also been established in our groups.[29]

Although the transition-metal-catalyzed click polymerizations are powerful, they also suffer from notable disadvantages. For example, some organometallic catalysts such as Ru(II) complexes are expensive and cytotoxic.[30,31] Moreover, the metallic residues are difficult to sweep away totally from the polymeric products, which might deteriorate the optoelectrical properties of products and cause cytotoxicity in biologic applications.[32] In addition, several resultant polymers generated by Cu(I)-catalyzed AACPs encounter the solubility problem due to the coordination of copper ions with the formed triazoles.[33] Therefore, minimal use or no use of the transition-metal catalyst in the click polymerization is highly desired.

To solve aforementioned problems, our research groups have developed the supported Cu(I), such as CuI@A-21 and CuI@PS-Phen-catalyzed AACPs and metal-free click polymerizations (MFCPs).[32,34−46] However, these AACPs still have plenty of room to improve. For example, the polymeric products yielded from the supported Cu(I)-catalyzed AACPs still suffer from the copper residue problem, although their amount is greatly decreased. For MFCPs, the activated monomers are indispensable, and the regioregularities of the resultant PTAs are hard to reach 100%. Moreover, the MFCPs for the preparation of 1,5-regioregular PTAs are quite limited. Among the scanty reports, such polymers could be synthesized via a tetramethylammonium hydroxide (NMe_4OH)-mediated click polymerization of aromatic diynes and aromatic diazides.[47] It should be noted that NMe_4OH is inconvenient for use because it is stored as a 25 wt % aqueous solution. Because the formed hydrophobic polymer is incompatible with

Received: March 27, 2019
Revised: May 22, 2019
Published: June 13, 2019

DOI: 10.1021/acs.macromol.9b00620
Macromolecules 2019, 52, 4713−4720

water, the solubility of polymers will be deteriorated to some extent.

Compared with ionic NMe_4OH, the uncharged organic phosphazene superbase, particularly *t*-BuP_4, has some remarkable virtues, such as highly enhanced basicity, good solubility in nonpolar solvents, hyposensitivity to oxygen and moisture, and excellent thermal stability.[48] Thus, this superbase often serves as catalyst for the construction of multifarious copolymers via ring-opening polymerizations.[49−53] According to the hypothetic mechanism of acetylide nucleophile attacking terminal nitrogen of azide,[54] *t*-BuP_4 might be able to mediate the azide−alkyne polymerization to generate 1,5-regioregular PTAs. Indeed, after systematical optimization of the polymerization conditions, soluble and thermally stable 1,5-regioregular PTAs with high molecular weights were obtained in high yields by the *t*-BuP_4-mediated AACP, which enriches the family of click polymerization. Moreover, according to our previous study, the variation in the regioregularities of PTA will lead to difference in its properties.[25,55] We thus further investigated the structure−property relationship of the resultant 1,5-regioregular PTAs with their 1,4-regioregular counterpart, which was prepared by the typical Cu(I)-catalyzed AACP using the same diyne and diazide monomers. The results show that 1,5- and 1,4-regioregular PTAs show distinct difference in the thermal stability, refractive index, and photophysical and electrochemical properties.

RESULTS AND DISCUSSION

Click Polymerization. To establish this new phosphazene base of *t*-BuP_4-mediated AACP, we systematically optimized the reaction conditions using **1a** and **2a** as model monomers under nitrogen (Scheme 1). First, the effect of *t*-BuP_4 amount

Scheme 1. *t*-BuP_4-Mediated Click Polymerizations of Diazides 1 and Diynes 2

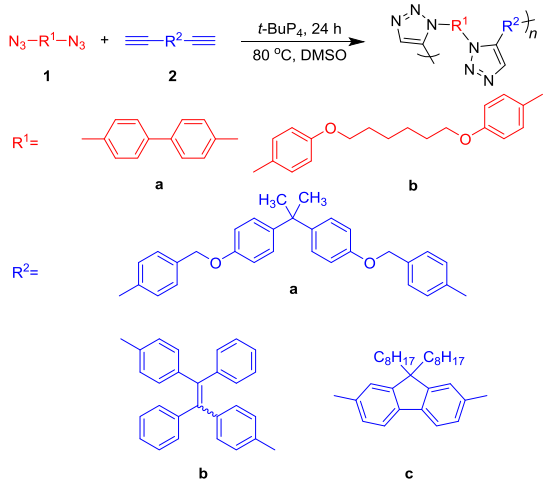

on the polymerization was investigated (Table 1). The weight-average molecular weight (M_w) values and yields of the products enhanced gradually when the concentration of *t*-BuP_4 increased from 10 to 50 mol %. Further increasing the loading amount of *t*-BuP_4 had a little effect on M_w and yield of the product. Hence, we fixed the *t*-BuP_4 concentration to 50 mol % for the optimal quantity. It is worth noting that the phosphazene base could be removed from the product during the precipitation process.

Table 1. Effect of *t*-BuP_4 Concentration on the Click Polymerization of 1a and 2a[a]

entry	*t*-BuP_4 (mol %)	yield (%)	M_w[b]	$Đ$[b]
1	75	71	4700	1.21
2	50	73	5300	1.16
3	25	13	3800	1.30
4	10	2	2400	1.11

[a]Carried out in DMSO at 25 °C under nitrogen for 24 h at a monomer concentration of 0.05 M. [b]Estimated by APC using THF as an eluant on the basis of polystyrene (PS) calibration; M_w = weight-average molecular weight; polydispersity index ($Đ$) = M_w/M_n; M_n = number-average molecular weight.

Next, the effect of reaction temperature on the click polymerization was studied, and the results are summarized in Table 2. With the increase of temperature from 25 to 80 °C,

Table 2. Effect of Reaction Temperature on the Click Polymerization of 1a and 2a[a]

entry	T (°C)	yield (%)	M_w[b]	$Đ$[b]
1[c]	25	73	5300	1.16
2	60	96	6900	1.41
3	80	98	7500	1.40
4	100	97	5100	1.33

[a]Carried out in DMSO for 24 h under nitrogen at a monomer concentration of 0.05 M, [*t*-BuP_4]/[**1a**] = 0.5. [b]Estimated by APC using THF as an eluant on the basis of PS calibration; M_w = weight-average molecular weight; $Đ$ = M_w/M_n; M_n = number-average molecular weight. [c]Data taken from Table 1, entry 2.

the M_w and polydispersity indices ($Đ$) and yields of products increased. A polymer with a M_w of 7500 and a $Đ$ of 1.40 could be obtained in 98% yield when the temperature was 80 °C. However, M_w decreased with further elevation of the reaction temperature. Thus, 80 °C was chosen as the optimal temperature.

After confirming the optimal temperature, we screened the reaction solvents. The experimental results showed that the M_w values, yields and fraction of 1,5-regioisomer ($F_{1,5}$) of PTAs produced in dimethyl sulfoxide (DMSO) and dimethylformamide (DMF) are higher than those in 1,4-dioxane and toluene, indicating that high polar solvents facilitate this click polymerization (Table 3). Although M_w of the polymer was little lower, slightly higher $F_{1,5}$ and yield of the product could be obtained when the polymerization was performed in DMSO

Table 3. Effect of Solvent on the Click Polymerization of 1a and 2a[a]

entry	solvent	yield (%)	M_w[b]	$Đ$[b]	$F_{1,5}$[c] (%)
1[d]	DMSO	98	7500	1.40	89
2	DMF	96	9000	1.53	81
3	1,4-dioxane	44	2200	1.12	53
4	toluene	35	2300	1.14	57

[a]Carried out at 80 °C for 24 h under nitrogen at a monomer concentration of 0.05 M, [*t*-BuP_4]/[**1a**] = 0.5. [b]Estimated by APC using THF as an eluant on the basis of PS calibration; M_w = weight-average molecular weight; $Đ$ = M_w/M_n; M_n = number-average molecular weight. [c]Fraction of the 1,5-regioisomer determined by ^{1}H NMR. [d]Data taken from Table 2, entry 3.

DOI: 10.1021/acs.macromol.9b00620
Macromolecules 2019, 52, 4713−4720

than in DMF. Thus, DMSO was adopted as the suitable solvent.

Furthermore, we followed the time course of the click polymerization. When the reaction time was prolonged from 6 to 24 h, M_w of polymers increased gradually, while their yields remained roughly constant (Table 4). Further extending the reaction time caused slight decrease in M_w of the product. Therefore, 24 h was used for further polymerization.

Table 4. Time Course of the Click Polymerization of 1a and 2a[a]

entry	t (h)	yield (%)	M_w[b]	$Đ$[b]
1	6	98	4700	1.36
2	12	96	4900	1.41
3	18	95	5300	1.36
4[c]	24	98	7500	1.40
5	30	96	5100	1.38

[a]Carried out in DMSO at 80 °C under nitrogen at a monomer concentration of 0.05 M, [t-BuP$_4$]/[**1a**] = 0.5. [b]Estimated by APC using THF as an eluant on the basis of PS calibration; M_w = weight-average molecular weight; $Đ$ = M_w/M_n; M_n = number-average molecular weight. [c]Data taken from Table 3, entry 1.

Afterward, the effect of the generation of the phosphazene base on the polymerization results was examined. Generally, the higher generation of the phosphazene base corresponds to the stronger basicity.[44] As shown in Table 5, the M_w values and

Table 5. Effect of the Generation of the Phosphazene Base on the Click Polymerization of 1a and 2a[a]

entry	organic base	yield (%)	M_w[b]	$Đ$[b]
1	t-BuP$_1$	trace	1400	1.12
2	t-BuP$_2$	86	3300	1.24
3[c]	t-BuP$_4$	98	7500	1.40

[a]Carried out in DMSO at 80 °C under nitrogen for 24 h at a monomer concentration of 0.05 M, [phosphazene base]/[**1a**] = 0.5. [b]Estimated by APC using THF as an eluant on the basis of PS calibration; M_w = weight-average molecular weight; $Đ$ = M_w/M_n; M_n = number-average molecular weight. [c]Data taken from Table 4, entry 4.

yields of PTAs greatly increased when the generation of the phosphazene base enhanced, suggesting that the basicity of the phosphazene base has a significant influence on the click polymerization. Therefore, we kept using t-BuP$_4$ as the polymerization base.

At last, we monitored the monomer concentration. With the increase of monomer concentration from 0.05 to 0.20 M, the M_w and $Đ$ values of the products progressively increased (Table 6). Further enhancement of the monomer concentration to 0.25 M helped less in increasing M_w and yield of the product. Hence, 0.20 M was chosen as the suitable monomer concentration.

By using these optimized conditions, we polymerized other diynes and diazides to test the universality and robustness of this superbase-mediated click polymerization (Table 7). All polymerizations propagated smoothly, and soluble polymers with high M_w (up to 26 600) and high regioregularities ($F_{1,5}$ in the range of 87−100%) were produced in excellent yields (up to 99%). These results manifest the universality of this powerful and efficient click polymerization. Furthermore, the resultant polymers are also thermally stable, and the temperatures of theirr 5% weight loss are higher than 305 °C (Figure S1).

Table 6. Effect of Monomer Concentration on the Click Polymerization of 1a and 2a[a]

entry	C (M)	yield (%)	M_w[b]	$Đ$[b]
1[c]	0.05	98	7500	1.40
2	0.15	98	8300	1.42
3	0.20	95	9200	1.50
4	0.25	94	9100	1.56

[a]Carried out in DMSO at 80 °C under nitrogen for 24 h, [t-BuP$_4$]/[**1a**] = 0.5. [b]Estimated by APC using THF as an eluant on the basis of PS calibration; M_w = weight-average molecular weight; $Đ$ = M_w/M_n; M_n = number-average molecular weight. [c]Data taken from Table 5, entry 3.

Table 7. Click Polymerization of Diazides 1 and Diynes 2[a]

polymer	monomer	yield (%)	M_w[b]	$Đ$[b]	$F_{1,5}$[c] (%)
PI[d]	**1a** + **2a**	95	9200	1.50	90
PII	**1a** + **2b**	98	9300	1.42	100
PIII	**1a** + **2c**	94	20 800	2.21	91
PIV	**1b** + **2a**	97	9600	1.44	87
PV	**1b** + **2b**	99	12 000	1.43	100
PVI	**1b** + **2c**	98	26 600	2.04	100

[a]Carried out in DMSO at 80 °C under nitrogen for 24 h at a monomer concentration of 0.20 M, [t-BuP$_4$]/[**1**] = 0.5. [b]Estimated by APC using THF as an eluant on the basis of PS calibration; M_w = weight-average molecular weight; $Đ$ = M_w/M_n; M_n = number-average molecular weight. [c]Fraction of the 1,5-regioisomer determined by ^{1}H NMR. [d]Data taken from Table 6, entry 3.

Structure Characterization. Benefited from the excellent solubility of the resultant polymers, their structures were characterized by spectroscopy techniques. The Fourier transform infrared (FT-IR) spectra of PI as well as its monomers **1a** and **2a** are shown in Figure 1 as an example. The stretching

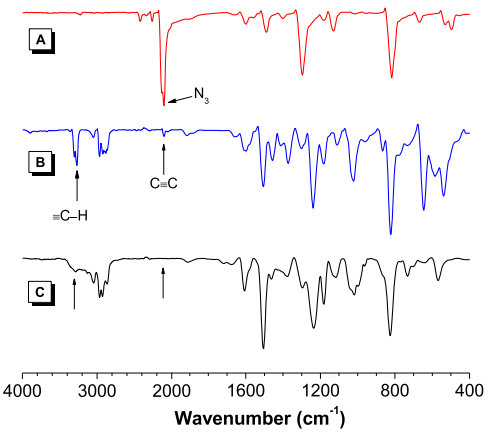

Figure 1. FT-IR spectra of **1a** (A), **2a** (B), and PI (C).

vibration of $-N_3$ of **1a** was peaked at 2101 cm^{-1}, and C≡C and ≡C−H vibration bands of **2a** appeared at 2107 and 3270 cm^{-1}, respectively. All these characteristic peaks in the spectrum of PI became very weak or almost vanished, suggesting that most of ethynyl and azide groups have been consumed. Similar results were observed in the FT-IR spectra of PII−PVI (Figures S2−S6).

The nuclear magnetic resonance (NMR) spectroscopy could provide more detail information about the structures of PTAs.

DOI: 10.1021/acs.macromol.9b00620
Macromolecules 2019, 52, 4713−4720

Owing to the NMR spectra of 1,5-regioregular PTAs that enjoy higher resolution in DMSO-d_6 than that in $CDCl_3$, ^1H and ^{13}C NMR spectra of **PI**–**PVI** were measured in DMSO-d_6.[29] Figure 2 shows the ^1H NMR spectra of **PI** as well as its

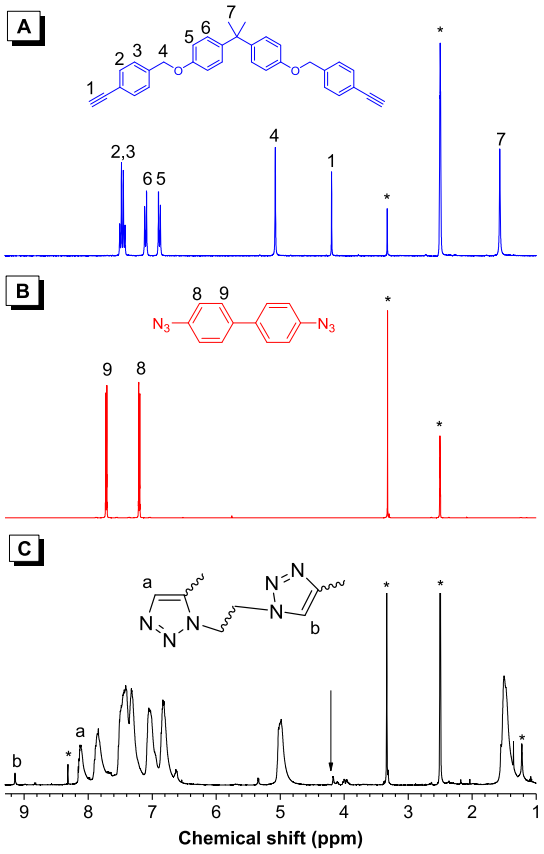

Figure 2. ^1H NMR spectra of **2a** (A), **1a** (B), and **PI** (C) in DMSO-d_6. The solvent peaks are marked with asterisks.

monomers **1a** and **2a** as a representative example. The ethynyl proton of **2a** resonating at δ 4.20 became much weaker in the spectrum of **PI**. Furthermore, new peaks corresponding to 1,4- and 1,5-regioisomeric triazoles appeared at δ 9.15 and 8.12, respectively. The fraction of 1,5-regioisomer of **PI** was thus calculated to be 90% from the integrals. Similar results were obtained in the ^1H NMR spectra of **PII**–**PVI** (Figures S7–S11). It should be noted that $F_{1,5}$ values of other PTAs are higher than 87%, and only the resonant protons of 1,5-regioisomers were recorded in **PII**, **PV**, and **PVI**, demonstrating that this click polymerization could furnish products with high regioregularities.

^{13}C NMR spectra further confirmed the occurrence of the click polymerization and the structures of the resultant polymers. Compared with monomer **2a**, the ethynyl carbon of ≡C– and ≡CH resonated at δ 83.77 and 81.33 in the spectrum of **PI**, respectively, which became much weaker (Figure S12). Similar results were obtained in the ^{13}C NMR spectra of **PII**–**PVI** (Figures S13–S17). These analysis results suggest that efficient and regioselective *t*-BuP_4-mediated AACP has been successfully established.

Structure–Property Relationship Investigation. To figure out the structure–property relationship of PTAs with different regioregularities, 1,5-regioregular PTA **PVI′** and 1,4-regioregular one **PVII** (Scheme 2) with a M_w of 13 800 and

Scheme 2. Cu(PPh_3)$_3$Br-Catalyzed Click Polymerization of Diazide 1b and Diyne 2c

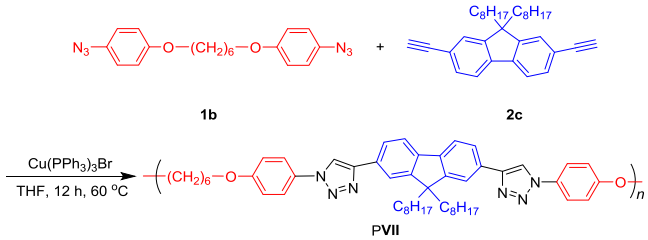

10 500 were synthesized by the *t*-BuP_4-mediated and Cu(PPh_3)$_3$Br-catalyzed click polymerizations of **1b** and **2c** under their optimal conditions, respectively. Their structures were fully characterized by the FT-IR and ^1H and ^{13}C NMR spectroscopy methods, and satisfactory results were obtained (Figures S18–S23). The thermal property investigation (Figure S24) and refractive index measurement (Figure S25) of **PVI′** and **PVII** show a similar trend with our reported conclusions that the thermal decomposion temperature, glass transition temperature, and refractive index values of 1,4-regioregular PTA are higher than that of the 1,5-regioregular one.[56]

Because the resultant PTAs contain the fluorenyl moiety, we thus studied their photophysical properties. The absorption spectra of **PVI′** and **PVII** in tetrahydrofuran (THF) with a concentration of 10^{-5} M are illustrated in Figure 3A. The absorption maxima of **PVII** was recorded at 332 nm, which is 8 nm red-shifted in comparison with that of **PVI′** (324 nm). Moreover, the spectrum of **PVII** showed shoulder peaks at 343 nm, while no such fine structural absorption was observed in the spectrum of **PVI′**. The results indicate that **PVII** possesses a better conjugated and planar conformation and stronger noncovalent interactions of polymer chains than those of **PVI′**.[57–59] More obvious difference of the absorption spectra of **PVI′** and **PVII** could be observed in their aggregate states upon addition of poor solvent of water into their THF solutions. As shown in Figure 3B,C, increasing the water fraction impacted a negligible effect on the absorption spectra of **PVI′**, while a notable change was found in that of **PVII**. Furthermore, with increasing water fraction, the shoulder peak in the spectrum of **PVII** gradually intensified and red-shifted probably because its planar structure, might facilitate the strong intermolecular interaction upon aggregation. A similar phenomenon could be observed in the densification processes (Figure S26A).

To further exemplify the different aggregation features of **PVI′** and **PVII**, their photoluminescence (PL) spectra and absolute fluorescence quantum yields (Φ_F) in THF/water mixtures with different water fractions were measured. As can be seen from Figure 4, the THF solution of **PVII** emitted strongly with a Φ_F value of 41.6%. However, it decreased dramatically with addition of water, demonstrative of a typical aggregation-caused quenching effect. The Φ_F value of **PVI′** in THF solution was measured to be only 12.6%. Upon increasing the water content, its descending degree of Φ_F was much lower than that of **PVII**. Similar results were perceived in their densification courses (Figure S26B,C). These behaviors might ascribe to the difference in their structural conformations,[29] suggestive of the stronger π–π stacking interaction of the planar conjugated backbone of **PVII**.

DOI: 10.1021/acs.macromol.9b00620
Macromolecules 2019, 52, 4713–4720

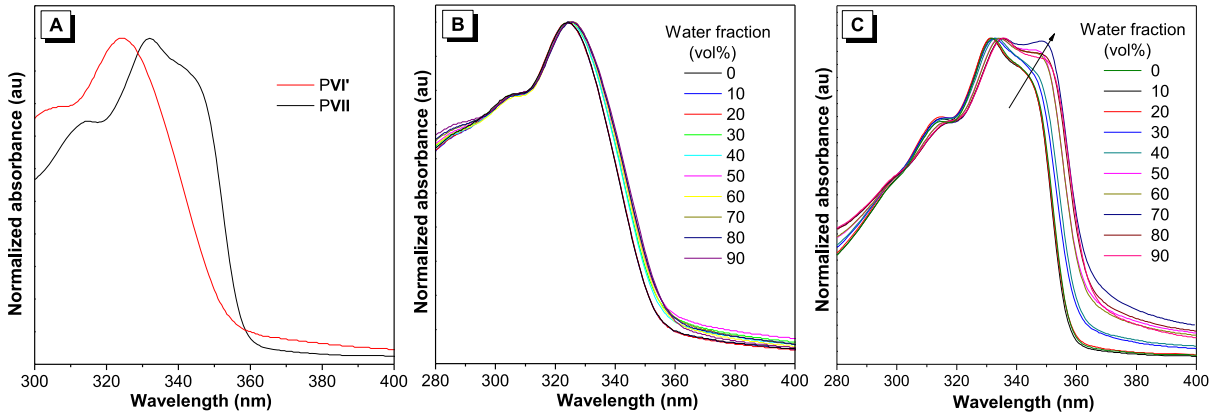

Figure 3. UV−vis absorption spectra of **PVI′** and **PVII** in THF solutions (A), **PVI′** (B), and **PVII** (C) in THF/water mixtures with different water fractions, polymer concentration: 10^{-5} M.

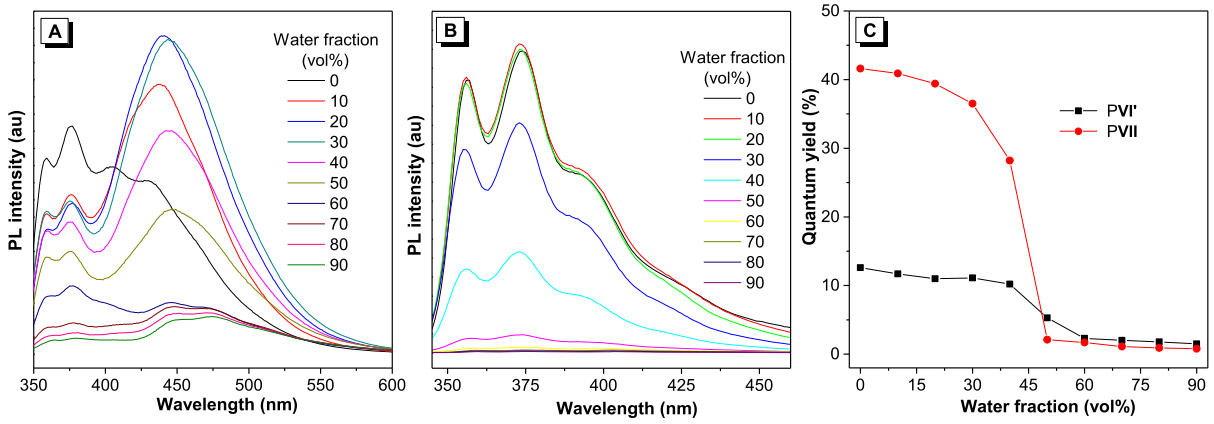

Figure 4. PL spectra of **PVI′** (A) and **PVII** (B) in THF/water mixtures with different water fractions; concentration: 10^{-5} M; excitation wavelengths: 324 nm for **PVI′** and 332 nm for **PVII**. (C) Plots of PL quantum yields vs water fraction in THF/water mixtures with different water fractions.

To gain a deep insight into the structures of **PVI′** and **PVII**, their geometries and spatial distributions of the highest occupied molecular orbitals (HOMOs) and the lowest unoccupied molecular orbitals (LUMOs) were calculated by employing the density functional theory method at the B3LYP/6-31G(d) level. To simplify the calculation, one-repeating units, namely, **PVI′-M** and **PVII-M** were used. As illustrated in Figure 5, **PVI′-M** adopts a twisted conformation, whereas **PVII-M** is more planar. Moreover, the HOMOs and LUMOs of **PVI′-M** and **PVII-M** are mostly located at fluorenyl and triazole rings. Twisted conformation of **PVI′** weakens the electronic coupling between the polymer chains, which is unfavorable for the π-electron delocalization. Moreover, a slight narrower energy band gap of **PVII-M** (3.99 eV) than that of **PVI′-M** (4.16 eV) indicates the extended conjugation in the repeating units of **PVII** (Figure S27). Notably, the calculation was further confirmed by the electrochemical property measurement. As shown in Figure S28, the oxidation onset potentials (E^{ox}_{onset}) of **PVI′** and **PVII** were recorded to be 1.89 and 1.40 V by cyclic voltammetry, respectively.

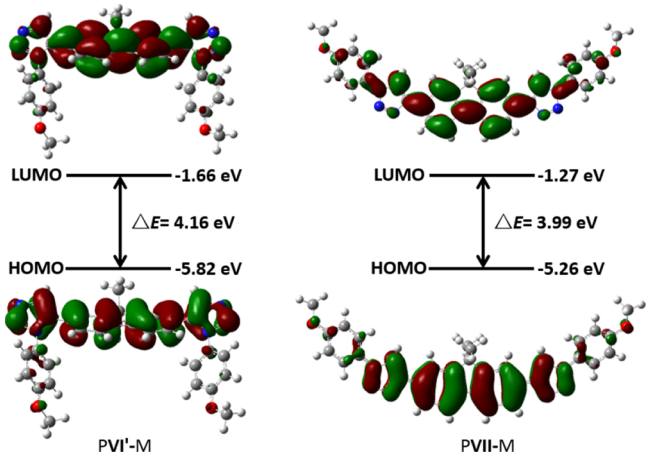

Figure 5. Calculated molecular conformation and orbital amplitude plots and energy levels of HOMOs and LUMOs of **PVI′-M** and **PVII-M**.

CONCLUSIONS

In summary, a new and efficient phosphazene base-mediated click polymerization of diynes and diazides was successfully developed, and soluble and thermally stable 1,5-regioregular PTAs with high M_w were obtained in high yields. Although 1,4- and 1,5-regioregular PTAs possess similar composition, their properties are quite different. The former possesses higher thermal stability and refractive indices than those of the latter. Moreover, they also show remarkable difference in the photophysical properties owing to their different structural conformations. The twisted structure of 1,5-regioregular PTA shows poorer conjugation and lower Φ_F in solution than those

DOI: 10.1021/acs.macromol.9b00620
Macromolecules 2019, 52, 4713−4720

of the planar 1,4-regioregular one. Thus, this work not only provides a new method for the construction of 1,5-regioregular PTAs but also offers a deeper insight into the structure−property relationship of PTAs, which will further guide the design of triazole-based functional materials.

EXPERIMENTAL SECTION

Materials. Phosphazene bases (*t*-BuP_1, *t*-BuP_2, and *t*-BuP_4) and Cu(PPh_3)$_3$Br were purchased from Sigma-Aldrich and used as received without further purification. THF and toluene were distilled under nitrogen at normal pressure from sodium benzophenone ketyl immediately prior to use. DMSO, DMF, and 1,4-dioxane were of extra-dry grade.

Instruments. The FT-IR spectra were collected on a Bruker Vector 22 spectrometer (KBr disks). The ^{1}H and ^{13}C NMR spectra were measured on a Bruker ADVANCE2B spectrometer in DMSO-d_6 and $CDCl_3$ using tetramethylsilane (TMS, δ = 0) as internal reference. The weight- and number-average molecular weights (M_w and M_n) and polydispersity indices ($Đ$, M_w/M_n) of the polymers were estimated by a Waters advanced polymer chromatography (APC) system equipped with a photodiode array detector, using monodisperse polystyrene as calibration and THF as an eluant at a flow rate of 0.5 mL/min. Thermogravimetric analysis measurements were carried out on PerkinElmer TGA 7 under dry nitrogen at a heating rate of 20 °C/min. Differential scanning calorimetry analysis was performed on a DSCAQ20 apparatus at a heating rate of 10 °C/min under dry nitrogen. UV−vis absorption spectra were recorded on a Shimadzu UV-2600 spectrophotometer. PL spectra were measured on a Horiba FluoroMax-4 spectrofluorometer. Absolute fluorescence quantum yields were recorded on a Hamamatsu absolute PL quantum yield spectrometer C11347 Quantaurus-QY. The fluorescence lifetime was determined by using the Quantaurus-Tau time-resolved spectrometer C11367 of Hamamatsu. The refractive index values were determined on a J.A. Woollam V-VASE variable angle ellipsometry measurement system. The polymer films were prepared by spin-coating on crystalline silicon with 1,2-dichloroethane as solvent. The Cauchy dispersion law was applied to analyze the polymer layers from the visible to the IR spectroscopy region. Cyclic voltammetry was carried out on a CHI610EA14297 electrochemical workstation with the platinum electrode and the saturated calomel electrode as the working electrode and the reference electrode, respectively, in dichloromethane solution with 0.1 M tetrabutylammonium hexafluorophosphate as the supporting electrolyte at a scan rate of 50 mV/s.

Polymerization. Unless otherwise stated, all the polymerizations of diazides **1** and diynes **2** were conducted under nitrogen using standard Schlenk techniques. The typical experimental procedure for the click polymerization is given below.

Phosphazene Base-Mediated Click Polymerization. Diazide monomer **1a** (23.6 mg, 0.1 mmol) and diyne monomer **2a** (45.6 mg, 0.1 mmol) were added into a 10 mL Schlenk tube, after evacuating and refilling with nitrogen thrice; *t*-BuP_4 (62.5 μL, 0.05 mmol) and extra-dry DMSO (0.5 mL) were injected to dissolve the monomers. The mixture was stirred at 80 °C for 24 h. Afterward, the resulting solution was diluted with 50 mL of $CHCl_3$ and washed with water thrice. The organic phase was concentrated by a rotary evaporator under reduced pressure. The residue was diluted with 5 mL $CHCl_3$ and added dropwise to 200 mL hexane through a cotton filter under stirring. The precipitates were filtered and washed with hexane several times and dried under vacuum at 40 °C to a constant weight.

Characterization Data of ***PI.*** A dark yellow powder was obtained in 95% yield. M_w: 9200; $Đ$: 1.50. FT-IR (KBr disk), ν (cm^{-1}): 2930, 1604, 1507, 1237, 1180, 1018, 824. ^{1}H NMR (500 MHz, DMSO-d_6), δ (TMS, ppm): 9.14 (the proton of 1,4-disubstituted triazole), 8.12 (the proton of 1,5-disubstituted triazole), 7.85−6.83 (Ar-*H*), 4.99 (CH_2), 1.49 (CH_3). ^{13}C NMR (125 MHz, DMSO-d_6), δ (ppm): 156.4, 143.3, 139.9, 138.9, 137.8, 136.2, 133.7, 132.2, 129.1, 128.4, 127.8, 126.5, 125.9, 114.5, 69.1, 41.6, 30.9.

Characterization Data of ***PII.*** A yellow powder was obtained in 98% yield. M_w: 9300; $Đ$: 1.42. FT-IR (KBr disk), ν (cm^{-1}): 3047, 1605, 1498, 1234, 980, 826, 697. ^{1}H NMR (500 MHz, DMSO-d_6), δ (TMS, ppm): 7.98 (the proton of 1,5-disubstituted triazole), 7.76−6.83 (Ar-*H*). ^{13}C NMR (125 MHz, DMSO-d_6), δ (ppm): 144.1, 142.7, 140.9, 139.6, 137.6, 136.0, 133.6, 131.5, 131.0, 127.2, 126.3, 124.8, 114.3.

Characterization Data of ***PIII.*** A dark yellow powder was obtained in 94% yield. M_w: 20 800; $Đ$: 2.21. FT-IR (KBr disk), ν (cm^{-1}): 2921, 2839, 1502, 1454, 1238, 823. ^{1}H NMR (500 MHz, DMSO-d_6), δ (TMS, ppm): 9.14 (the proton of 1,4-disubstituted triazole), 8.14 (the proton of 1,5-disubstituted triazole), 7.99−6.82 (Ar-*H*), 1.55−0.22 (CH_2). ^{13}C NMR (125 MHz, DMSO-d_6), δ (ppm): 139.3, 138.1, 136.5, 134.0, 128.7, 125.8, 123.3, 121.6, 114.3, 54.9, 31.6, 29.1, 22.6, 13.9.

Characterization Data of ***PIV.*** A light yellow powder was obtained in 97% yield. M_w: 9600; $Đ$: 1.44. FT-IR (KBr disk), ν (cm^{-1}): 2929, 1605, 1506, 1241, 1018, 826. ^{1}H NMR (500 MHz, DMSO-d_6), δ (TMS, ppm): 9.14 (the proton of 1,4-disubstituted triazole), 8.08 (the proton of 1,5-disubstituted triazole), 7.40−6.63 (Ar-*H*), 5.01 (CH_2), 3.99 (CH_2), 1.72−1.45 (CH_2). ^{13}C NMR (125 MHz, DMSO-d_6), δ (ppm): 159.7, 156.3, 143.2, 138.7, 137.8, 133.3, 129.4, 128.7, 128.0, 126.4, 115.6, 114.4, 69.0, 68.3, 41.9, 31.3, 29.1, 25.7.

Characterization Data of ***PV.*** A light yellow powder was obtained in 99% yield. M_w: 12 000; $Đ$: 1.43. FT-IR (KBr disk), ν (cm^{-1}): 2921, 1509, 1245, 834, 698. ^{1}H NMR (500 MHz, DMSO-d_6), δ (TMS, ppm): 8.01 (the proton of 1,5-disubstituted triazole), 7.14−6.86 (Ar-*H*), 3.99 (CH_2), 1.68−1.43 (CH_2). ^{13}C NMR (125 MHz, DMSO-d_6), δ (ppm): 159.6, 144.0, 142.9, 141.0, 137.5, 133.3, 131.2, 129.4, 128.3, 127.5, 125.0, 115.5, 68.4, 28.9, 25.8.

Characterization Data of ***PVI.*** A dark yellow powder was obtained in 98% yield. M_w: 26 600; $Đ$: 2.04. FT-IR (KBr disk), ν (cm^{-1}): 2929, 2850, 1604, 1511, 1465, 1302, 1245, 1053, 829. ^{1}H NMR (500 MHz, DMSO-d_6), δ (TMS, ppm): 8.13 (the proton of 1,5-disubstituted triazole), 7.87−6.93 (Ar-*H*), 3.94 (CH_2), 1.71−0.18 (CH_2). ^{13}C NMR (125 MHz, DMSO-d_6), δ (ppm): 159.6, 150.7, 140.8, 138.1, 133.1, 129.9, 127.7, 125.9, 123.2, 121.5, 115.3, 114.4, 68.2, 31.6, 29.2, 25.7, 22.6, 14.5.

Cu(PPh_3)$_3$Br-Catalyzed AACP. Diazide monomer **1b** (35.2 mg, 0.1 mmol), diyne monomer **2c** (43.8 mg, 0.1 mmol), and Cu(PPh_3)$_3$Br (9.3 mg, 0.01 mmol) were added into a 10 mL Schlenk tube. After evacuating and refilling with nitrogen thrice, 2 mL freshly distilled THF was injected to dissolve the monomers. The mixture was stirred at 60 °C for 12 h. Afterward, the resulting solution was diluted with 5 mL THF and added dropwise to 200 mL hexane through a cotton filter under stirring. The precipitates were collected by filtration and washed with hexane several times and dried under vacuum at 40 °C to a constant weight.

Characterization Data of ***PVII.*** A yellow powder was obtained in 78% yield. M_w: 10 500; $Đ$: 1.29. FT-IR (KBr disk), ν (cm^{-1}): 2929, 2847, 1513, 1459, 1252, 1039, 826. ^{1}H NMR (500 MHz, $CDCl_3$), δ (TMS, ppm): 8.19 (the proton of 1,4-disubstituted triazole), 7.99−7.04 (Ar-*H*), 4.06 (CH_2), 2.10−0.67 (CH_2). ^{13}C NMR (125 MHz, $CDCl_3$), δ (ppm): 159.4, 151.9, 148.8, 141.1, 130.6, 129.2, 124.7, 122.2, 120.2, 118.0, 115.5, 68.5, 55.7, 40.7, 31.9, 29.4, 30.0, 25.8, 22.8, 24.1, 14.2.

ASSOCIATED CONTENT

Supporting Information

The Supporting Information is available free of charge on the ACS Publications website at DOI: 10.1021/acs.macromol.9b00620.

Detailed synthetic routes to monomers **1** and **2**; FT-IR and ^{1}H and ^{13}C NMR spectra of **1**, **2**, and **PI**−**PVII**; and TGA curves, DSC curves, RI values, dihedral angles, and cyclic voltammograms of **PVI′** and **PVII** (PDF)

DOI: 10.1021/acs.macromol.9b00620
Macromolecules 2019, 52, 4713−4720

AUTHOR INFORMATION

Corresponding Authors

*E-mail: msqinaj@scut.edu.cn (A.Q.).
*E-mail: tangbenz@ust.hk (B.Z.T.).

ORCID

Anjun Qin: 0000-0001-7158-1808
Ben Zhong Tang: 0000-0002-0293-964X

Notes

The authors declare no competing financial interest.

ACKNOWLEDGMENTS

This work was financially supported by the National Natural Science Foundation of China (21788102, 21525417, and 21490571), the National Program for Support of Top-Notch Young Professionals, the Natural Science Foundation of Guangdong Province (2016A030312002), the Fundamental Research Funds for the Central Universities (2015ZY013), and the Innovation and Technology Commission of Hong Kong (ITC-CNERC14S01).

REFERENCES

(1) Lowe, A. B. Thiol-ene "click" reactions and recent applications in polymer and materials synthesis: a first update. *Polym. Chem.* **2014**, *5*, 4820−4870.
(2) Li, K.; Liu, B. Water-Soluble Conjugated Polymers as the Platform for Protein Sensors. *Polym. Chem.* **2010**, *1*, 252−259.
(3) Martens, S.; Holloway, J. O.; Du Prez, F. E. Click and Click-Inspired Chemistry for the Design of Sequence-Controlled Polymers. *Macromol. Rapid Commun.* **2017**, *38*, 1700469.
(4) Dadashi-Silab, S.; Doran, S.; Yagci, Y. Photoinduced Electron Transfer Reactions for Macromolecular Syntheses. *Chem. Rev.* **2016**, *116*, 10212−10275.
(5) Matyjaszewski, K.; Xia, J. Atom Transfer Radical Polymerization. *Chem. Rev.* **2001**, *101*, 2921−2990.
(6) Xie, Z.; Wei, Y.; Zhao, X.; Li, Y.; Ding, S.; Chen, L. Facile Construction of Butadiynylene Based Conjugated Porous Polymers by Cost-Effective Glaser Coupling. *Mater. Chem. Front.* **2017**, *1*, 867−872.
(7) Kolb, H. C.; Finn, M. G.; Sharpless, K. B. Click Chemistry: Diverse Chemical Function from a Few Good Reactions. *Angew. Chem., Int. Ed.* **2001**, *40*, 2004−2021.
(8) Zhang, L.; Chen, X.; Xue, P.; Sun, H. H. Y.; Williams, I. D.; Sharpless, K. B.; Fokin, V. V.; Jia, G. Ruthenium-Catalyzed Cycloaddition of Alkynes and Organic Azides. *J. Am. Chem. Soc.* **2005**, *127*, 15998−15999.
(9) Majireck, M. M.; Weinreb, S. M. A Study of the Scope and Regioselectivity of the Ruthenium-Catalyzed [3 + 2]-Cycloaddition of Azides with Internal Alkynes. *J. Org. Chem.* **2006**, *71*, 8680−8683.
(10) Bock, V. D.; Hiemstra, H.; van Maarseveen, J. H. CuI-Catalyzed Alkyne-Azide "Click" Cycloadditions from a Mechanistic and Synthetic Perspective. *Eur. J. Org. Chem.* **2006**, 51−68.
(11) Braunschweig, A. B.; Dichtel, W. R.; Miljanić, O. Š.; Olson, M. A.; Spruell, J. M.; Khan, S. I.; Heath, J. R.; Stoddart, J. F. Modular Synthesis and Dynamics of a Variety of Donor-Acceptor Interlocked Compounds Prepared by Click Chemistry. *Chem.—Asian J.* **2007**, *2*, 634−647.
(12) Aprahamian, I.; Miljanić, O. Š.; Dichtel, W. R.; Kyosuke, I.; Takuma, Y.; Takashi, K.; Fraser, S. J. Clicked Interlocked Molecules. *Bull. Chem. Soc. Jpn.* **2007**, *80*, 1856−1869.
(13) Salisbury, C. M.; Cravatt, B. F. Click Chemistry-LED Advances in High Content Functional Proteomics. *QSAR Comb. Sci.* **2007**, *26*, 1229−1238.
(14) Qin, A.; Lam, J. W. Y.; Tang, B. Z. Click Polymerization. *Chem. Soc. Rev.* **2010**, *39*, 2522−2544.
(15) Qin, A.; Lam, J. W. Y.; Tang, B. Z. Click Polymerization: Progresses, Challenges, and Opportunities. *Macromolecules* **2010**, *43*, 8693−8702.
(16) Li, H.-k.; Sun, J.-z.; Qin, A.-j.; Tang, B. Z. Azide-Alkyne Click Polymerization: An Update. *Chin. J. Polym. Sci.* **2012**, *30*, 1−15.
(17) Wang, J.; Mei, J.; Zhao, E.; Song, Z.; Qin, A.; Sun, J. Z.; Tang, B. Z. Ethynyl-Capped Hyperbranched Conjugated Polytriazole: Click Polymerization, Clickable Modification, and Aggregation-Enhanced Emission. *Macromolecules* **2012**, *45*, 7692−7703.
(18) Qin, A.; Lam, J. W. Y.; Tang, L.; Jim, C. K. W.; Zhao, H.; Sun, J.; Tang, B. Z. Polytriazoles with Aggregation-Induced Emission Characteristics: Synthesis by Click Polymerization and Application as Explosive Chemosensors. *Macromolecules* **2009**, *42*, 1421−1424.
(19) Huang, D.; Qin, A.; Tang, B. Z. Hyperbranched Polymers Prepared by Alkyne-Based Click Polymerization. *Acta Polym. Sin.* **2017**, 178−199.
(20) Qiu, Z.; Han, T.; Lam, J. W. Y.; Tang, B. Z. Recent New Methodologies for Acetylenic Polymers with Advanced Functionalities. *Top. Curr. Chem.* **2017**, *375*, 70.
(21) Shi, Y.; Sun, J. Z.; Qin, A. Click polymerization: The Aurora of Polymer Synthetic Methodology. *J. Polym. Sci., Part A: Polym. Chem.* **2017**, *55*, 616−621.
(22) Wu, Y.-w.; Qin, A.-j.; Tang, B. Z. AIE-Active Polymers for Explosive Detection. *Chin. J. Polym. Sci.* **2017**, *35*, 141−154.
(23) Cao, X.; Shi, Y.; Gan, W.; Naguib, H.; Wang, X.; Graff, R. W.; Gao, H. Effect of Monomer Structure on the CuAAC Polymerization to Produce Hyperbranched Polymers. *Macromolecules* **2016**, *49*, 5342−5349.
(24) Cao, X.; Shi, Y.; Wang, X.; Graff, R. W.; Gao, H. Design a Highly Reactive Trifunctional Core Molecule to Obtain Hyperbranched Polymers with Over a Million Molecular Weight in One-Pot Click Polymerization. *Macromolecules* **2016**, *49*, 760−766.
(25) Han, J.; Zhu, D.; Gao, C. Fast Bulk Click Polymerization Approach to Linear and Hyperbranched Alternating Multiblock Copolymers. *Polym. Chem.* **2013**, *4*, 542−549.
(26) Tang, R.; Chen, H.; Zhou, S.; Xiang, W.; Tang, X.; Liu, B.; Dong, Y.; Zeng, H.; Li, Z. Dendronized Hyperbranched Polymers Containing Isolation Chromophores: Design, Synthesis and Further Enhancement of the Comprehensive NLO Performance. *Polym. Chem.* **2015**, *6*, 5580−5589.
(27) Li, Z.; Wu, W.; Li, Q.; Yu, G.; Xiao, L.; Liu, Y.; Ye, C.; Qin, J.; Li, Z. High-Generation Second-Order Nonlinear Optical (NLO) Dendrimers: Convenient Synthesis by Click Chemistry and the Increasing Trend of NLO Effects. *Angew. Chem., Int. Ed.* **2010**, *49*, 2763−2767.
(28) Chen, P.; Zhang, H.; Han, M.; Cheng, Z.; Peng, Q.; Li, Q.; Li, Z. Janus Molecules: Large Second-Order Nonlinear Optical Performance, Good Temporal Stability, Excellent Thermal Stability and Spherical Structure with Optimized Dendrimer Structure. *Mater. Chem. Front.* **2018**, *2*, 1374−1382.
(29) Qin, A.; Lam, J. W. Y.; Jim, C. K. W.; Zhang, L.; Yan, J.; Häussler, M.; Liu, J.; Dong, Y.; Liang, D.; Chen, E.; Jia, G.; Tang, B. Z. Hyperbranched Polytriazoles: Click Polymerization, Regioisomeric Structure, Light Emission, and Fluorescent Patterning. *Macromolecules* **2008**, *41*, 3808−3822.
(30) Lutz, J.-F. Copper-Free Azide-Alkyne Cycloadditions: New Insights and Perspectives. *Angew. Chem., Int. Ed.* **2008**, *47*, 2182−2184.
(31) Becer, C. R.; Hoogenboom, R.; Schubert, U. S. Click Chemistry Beyond Metal-Catalyzed Cycloaddition. *Angew. Chem., Int. Ed.* **2009**, *48*, 4900−4908.
(32) Wang, Q.; Chen, M.; Yao, B.; Wang, J.; Mei, J.; Sun, J. Z.; Qin, A.; Tang, B. Z. A Polytriazole Synthesized by 1,3-Dipolar Polycycloaddition Showing Aggregation-Enhanced Emission and Utility in Explosive Detection. *Macromol. Rapid Commun.* **2013**, *34*, 796−802.
(33) Karim, M. A.; Cho, Y.-R.; Park, J. S.; Kim, S. C.; Kim, H. J.; Lee, J. W.; Gal, Y.-S.; Jin, S.-H. Novel fluorene-based functional 'click

DOI: 10.1021/acs.macromol.9b00620
Macromolecules 2019, 52, 4713−4720

polymers' for quasi-solid-state dye-sensitized solar cells. *Chem. Commun.* **2008**, 1929−1931.
(34) Wu, H.; Li, H.; Kwok, R. T. K.; Zhao, E.; Sun, J. Z.; Qin, A.; Tang, B. Z. A Recyclable and Reusable Supported Cu(I) Catalyzed Azide-Alkyne Click Polymerization. *Sci. Rep.* **2014**, *4*, 5107.
(35) Wu, H.; Dong, W.; Wang, Z.; Yao, B.; Chen, M.; Sun, J.; Qin, A.; Tang, B. Z. An air-stable supported Cu(I) catalyst for azide-alkyne click polymerization. *Sci. China: Chem.* **2015**, *58*, 1748−1752.
(36) Qin, A.; Jim, C. K. W.; Lu, W.; Lam, J. W. Y.; Häussler, M.; Dong, Y.; Sung, H. H. Y.; Williams, I. D.; Wong, G. K. L.; Tang, B. Z. Click Polymerization: Facile Synthesis of Functional Poly(aroyltriazole)s by Metal-Free, Regioselective 1,3-Dipolar Polycycloaddition. *Macromolecules* **2007**, *40*, 2308−2317.
(37) Wei, Q.; Wang, J.; Shen, X.; Zhang, X.; Sun, J. Z.; Qin, A.; Tang, B. Z. Self-Healing Hyperbranched Poly(aroyltriazole)s. *Sci. Rep.* **2013**, *3*, 1093.
(38) Li, H.; Mei, J.; Wang, J.; Zhang, S.; Zhao, Q.; Wei, Q.; Qin, A.; Sun, J.; Tang, B. Z. Facile Synthesis of Poly(aroxycarbonyltriazole)s with Aggregation-Induced Emission Characteristics by Metal-Free Click Polymerization. *Sci. China: Chem.* **2011**, *54*, 611−616.
(39) Li, H.; Wang, J.; Sun, J. Z.; Hu, R.; Qin, A.; Tang, B. Z. Metal-Free Click Polymerization of Propiolates and Azides: Facile Synthesis of Functional Poly(aroxycarbonyltriazole)s. *Polym. Chem.* **2012**, *3*, 1075−1083.
(40) Li, H.; Li, L.; Wu, H.; Lam, J. W. Y.; Sun, J. Z.; Qin, A.; Tang, B. Z. Ferrocene-Based Poly(aroxycarbonyltriazole)s: Synthesis by Metal-Free Click Polymerization and Use as Precursors to Magnetic Ceramics. *Polym. Chem.* **2013**, *4*, 5537−5541.
(41) Li, H.; Wang, Z.; Li, J.; Zhao, E.; Sun, J. Z.; Lam, J. W. Y.; Qin, A.; Tang, B. Z. Facile Preparation of Light Refractive Poly(aroxycarbonyltriazole)s by Metal-Free Click Polymerization. *Macromol. Chem. Phys.* **2014**, *215*, 1036−1041.
(42) Li, H.; Wu, H.; Zhao, E.; Li, J.; Sun, J. Z.; Qin, A.; Tang, B. Z. Hyperbranched Poly(aroxycarbonyltriazole)s: Metal-Free Click Polymerization, Light Refraction, Aggregation-Induced Emission, Explosive Detection, and Fluorescent Patterning. *Macromolecules* **2013**, *46*, 3907−3914.
(43) Wang, Q.; Li, H.; Wei, Q.; Sun, J. Z.; Wang, J.; Zhang, X. A.; Qin, A.; Tang, B. Z. Metal-Free Click Polymerizations of Activated Azide and Alkynes. *Polym. Chem.* **2013**, *4*, 1396−1401.
(44) Wang, X.; Hu, R.; Zhao, Z.; Qin, A.; Tang, B. Z. Self-Healing Hyperbranched Polytriazoles Prepared by Metal-Free Click Polymerization of Propiolate and Azide Monomers. *Sci. China: Chem.* **2016**, *59*, 1554−1560.
(45) Meng, X.; Chen, H.; Xu, S.; Ma, Y. Metal-Free 1,3-Dipolar Cycloaddition Polymerization via Prearrangement of Azide and Alkyne in the Solid State. *CrystEngComm* **2014**, *16*, 9983−9986.
(46) Ni, B.-B.; Wang, C.; Wu, H.; Pei, J.; Ma, Y. Copper-Free Cycloaddition of Azide and Alkyne in Crystalline State Facilitated by Arene-Perfluoroarene Interactions. *Chem. Commun.* **2010**, *46*, 782−784.
(47) Liu, Y.; Wang, J.; Huang, D.; Zhang, J.; Guo, S.; Hu, R.; Zhao, Z.; Qin, A.; Tang, B. Z. Synthesis of 1,5-Regioregular Polytriazoles by Efficient NMe_4OH-Mediated Azide-Alkyne Click Polymerization. *Polym. Chem.* **2015**, *6*, 5545−5549.
(48) Kondo, Y. In *Superbases for Organic Synthesis: Guanidines, Amidines and Phosphazenes and Related Organocatalysts*, 1st ed.; Ishikawa, T., Ed.; John Wiley & Sons, Ltd.: Great Britain, 2009; Vol. *5*, p 145.
(49) Zhao, J.; Mountrichas, G.; Zhang, G.; Pispas, S. Thermoresponsive Core−Shell Brush Copolymers with Poly(propylene oxide)-block-poly(ethylene oxide) Side Chains via a "Grafting from" Technique. *Macromolecules* **2010**, *43*, 1771−1777.
(50) Yang, H.; Yan, M.; Pispas, S.; Zhang, G. Synthesis of Poly[(ethylene carbonate)-co-(ethylene oxide)] Copolymer by Phosphazene-Catalyzed ROP. *Macromol. Chem. Phys.* **2011**, *212*, 2589−2593.
(51) Yang, H.; Xu, J.; Pispas, S.; Zhang, G. Hybrid Copolymerization of ε-Caprolactone and Methyl Methacrylate. *Macromolecules* **2012**, *45*, 3312−3317.
(52) Zhao, J.; Pahovnik, D.; Gnanou, Y.; Hadjichristidis, N. One-pot synthesis of linear- and three-arm star-tetrablock quarterpolymers via sequential metal-free ring-opening polymerization using a "catalyst switch" strategy. *J. Polym. Sci., Part A: Polym. Chem.* **2015**, *53*, 304−312.
(53) Hu, S.; Zhao, J.; Zhang, G. Noncopolymerization Approach to Copolymers via Concurrent Transesterification and Ring-Opening Reactions. *ACS Macro Lett.* **2016**, *5*, 40−44.
(54) Kwok, S. W.; Fotsing, J. R.; Fraser, R. J.; Rodionov, V. O.; Fokin, V. V. Transition-Metal-Free Catalytic Synthesis of 1,5-Diaryl-1,2,3-Triazoles. *Org. Lett.* **2010**, *12*, 4217−4219.
(55) Zhao, E.; Li, H.; Ling, J.; Wu, H.; Wang, J.; Zhang, S.; Lam, J. W. Y.; Sun, J. Z.; Qin, A.; Tang, B. Z. Structure-Dependent Emission of Polytriazoles. *Polym. Chem.* **2014**, *5*, 2301−2308.
(56) Huang, D.; Liu, Y.; Qin, A.; Tang, B. Z. Structure-Property Relationship of Regioregular Polytriazoles Produced by Ligand-Controlled Regiodivergent Ru(II)-Catalyzed Azide-Alkyne Click Polymerization. *Macromolecules* **2019**, *52*, 1985−1992.
(57) Chen, Z.; Cai, P.; Chen, J.; Liu, X.; Zhang, L.; Lan, L.; Peng, J.; Ma, Y.; Cao, Y. Low Band-Gap Conjugated Polymers with Strong Interchain Aggregation and Very High Hole Mobility Towards Highly Efficient Thick-Film Polymer Solar Cells. *Adv. Mater.* **2014**, *26*, 2586−2591.
(58) Jheng, J.-F.; Lai, Y.-Y.; Wu, J.-S.; Chao, Y.-H.; Wang, C.-L.; Hsu, C.-S. Influences of the Non-Covalent Interaction Strength on Reaching High Solid-State Order and Device Performance of a Low Bandgap Polymer with Axisymmetrical Structural Units. *Adv. Mater.* **2013**, *25*, 2445−2451.
(59) Yang, C.; Orfino, F. P.; Holdcroft, S. A Phenomenological Model for Predicting Thermochromism of Regioregular and Non-regioregular Poly(3-alkylthiophenes). *Macromolecules* **1996**, *29*, 6510−6517.

DOI: 10.1021/acs.macromol.9b00620
Macromolecules 2019, 52, 4713−4720